*Agronomy Research* **13**(3), 629–638, 2015

# FEM based numerical simulation for heat treatment of the agricultural tools

R. Chotěborský[1] and M. Linda[2,*]

[1]Czech University of Life Sciences in Prague, Faculty of Engineering, Department of Material Science and Manufacturing Technology, Kamýcka 129, CZ-16521 Praha – Suchdol, Czech Republic
[2]Czech University of Life Sciences in Prague, Faculty of Engineering, Department of Electrical Engineering and Automation, Kamýcka 129, CZ-16521 Praha – Suchdol, Czech Republic; [*]Correspondence: linda@tf.czu.cz

**Abstract.** Quenching as a heat treatment method is commonly used to control the mechanical properties of steels. This article deals with the modelling and simulation of quenching of steel chisel using a multi–phase model. The process of the heat treatment is non stationary phase due to temperature variation with time. In this study, the problem of heat transfer in three dimensional phase was transformed into a two dimensional axisymmetric case. ElmerFem solver was used for the heat transfer through different cooling media such as water, oil and salt bath. The results from heat solver were used for austenite transformation modelling by applying Johnson–Mehl–Avrami–Kolmogorov equation in TTT diagram. The Scheill's decomposition was used for anisothermal transformation of austenite. The hardness prediction was done according to simple mixture rule where total hardness of the steel was calculated based on volume of the phases and their Vickers hardness.

**Key words:** numerical simulation, FEM, heat treatment, ElmerFEM.

## INTRODUCTION

Quenching is used as a heat treatment method for controlling the mechanical properties of steel such as tensile strength, toughness and hardness. The quenching process promotes the formation of different microstructures namely ferrite, pearlite, bainite and martensite that depend on the cooling rate as well as the chemical composition of the steel. The quenching application of the material is subjected to heat treatment above the austenitization temperature (approximately 900 °C) which involves continuous and rapid cooling in a quenching media such as water, air and oil. During quench hardening process, heat flux is rapidly transfered to the coolant which varies in time hence the HTC (heat transfer coefficient) cannot be calculated or measured by standard techniques. In such cases, the effective procedure is the formulation of the boundary inverse heat conduction (Telejko, 2004; Buczek & Telejko, 2013).

Constitutive modelling of the quenching process can be performed within the scope of standard generalized materials under the assumption that the thermodynamic state of the material can be completely defined by a finite number of state variables (Archambault & Azim, 1995; Fall et al., 2011; Hasan et al., 2010). Phase transformation

from austenite to martensite is non diffusive process meaning that the amount of volume fraction is only a function of temperature which can be described by the Koistinen–Marburger law (Eq. 1). On the other hand, microstructures such as ferrite, pearlite and bainite formations are diffusion controlled transformation which are time dependent. The diffusive transformation kinetics are described by Johnson–Mehl–Avrami–Koglomorov (JMAK) equation (Eq. 2). The evolution of these phases transformation can be predicted through an approximate solution using data from Time–Temperature–Transformation diagrams (TTT).

$$V_M = 1 - e^{-\alpha \times (M_s - T)} \tag{1}$$

$$V_{P,B} = 1 - e^{-k \times t^n} \tag{2}$$

where: $\alpha$ and $M_s$ are both constants determined by material type, $k$ is the overall rate constant that generally depends on temperature, $n$ is the Avrami's exponent (Kolmorgorov, 1937; Avrami, 1939a; Avrami, 1939b; Johnson & Mehl, 1939; Avrami, 1940a; Avrami, 1940b; Marder & Goldstein, 1984; Kirkaldy, 2007; Sinha et al., 2007).

This article describes the modelling and simulation of quenching of steel chisel using a multiphase constitutive model proposed by (Çetinel et al., 2000; Ferguson et al., 2005; Carlone et al., 2010).

## MATERIALS AND METHODS

The process of heat transfer during quenching of a steel chisel (Fig. 1) is nonstationary due to the variation of temperature with time. In this work the problem of heat transfer in a three dimensional phase was examined.

**Figure 1.** Real chisel computerization.

The nonstationary problem of heat transfer within a component in the quenching process is described mathematically by simple differentiation with respect to the volume. Based on that the heat transfer equation (Eq. 3) was derived as follows:

$$\frac{\partial}{\partial x}\left(k\frac{\partial T}{\partial x}\right) + \frac{\partial}{\partial y}\left(k\frac{\partial T}{\partial y}\right) + \frac{\partial}{\partial z}\left(k\frac{\partial T}{\partial z}\right) + Q = \rho \times c \times \frac{\partial T}{\partial t} \tag{3}$$

where: $k$ – thermal conductivity; $Q$ – is the inner heat–generation rate per unit volume; $T$ – temperatuure; $q$ – heat transfer coefficiente; $\rho$ – densitye; $c$ – heat capacitye; $t$ – time.

The Neumann boundary conditions were used for the simulation of the heat cycles in quenching media like air, water and oil whiles the heat flux was determined experimentally in cylinder shape samples by inverse methods (Telejko, 2004).

The equilibrium transformation temperatures during cooling were also determined experimentally by thermal analysis. The ferrite transformation started below the $A_{c3}$ temperature whiles the pearlite transformation occurred at the $A_{c1}$ temperature when a volume fraction of pro–eutectoid ferrite reached an equilibrium volume fraction. The bainite and martensite transformations occurred below bainite and martensite temperatures respectively. Table 1 gives the transformation temperatures of different steel samples.

**Table 1.** Transformation temperatures of different steel samples

| Temperature phase change | $A_{c3}=T_F$ (°C) | $A_{c1}=T_P$ (°C) | $T_B$ (°C) | $T_M$ (°C) |
|---|---|---|---|---|
| High boron steel – B1 | 810 | 741 | 606 | 382 |
| High boron steel – B2 | 830 | 743 | 593 | 411 |
| Boron27 | 840 | 675 | 525 | 335 |

**Table 2.** Chemical composition of different steel samples

| Chemical composition | C | Si | Ni | Cr | Mn | Mo | Cu |
|---|---|---|---|---|---|---|---|
| High boron steel – B1 | 0.6 | 0.3 | 0.05 | 0.4 | 0 | 0.01 | 0 |
| High boron steel – B2 | 0.3 | 0.3 | 1 | 1.5 | 0 | 0.05 | 0 |
| Boron27 | 0.2 | 0.2 | 0.1 | 0.3 | 1.3 | 0 | 0 |

The ElmerFEM solver (CSC – IT Center for Science (CSC), 2013) was used for calculation of thermal field of the steel samples. The simulation results were obtained as matrix of nodes and temperatures. Two kinds of mathematical models were used for deducing microstructure field from temperature field based on TTT (Time, Temperature, Transformation) curve which is used for kinetic transformation of austenite at constant temperature. In addition, CCT (Continuous Cooling Transformation) curve was used for kinetic transformation of austenite in water and oil quenching media (Smoljan, 2006; Malinowski et al., 2012).

The diffusional transformation reaction was based on equation (Eq. 2). The constants for these equations were determined from a nonlinear optimization of the experimental data. Table 2 shows the values used for the three transformation products resulting from a diffusion–controlled reaction of ferrite, pearlite and bainite. The temperature dependencies of constants were fitted by Gaussian function and these dependencies were used as input algorithm (Marder & Goldstein, 1984; Çetinel et al., 2000; Ferguson et al., 2005). The C–curves of a calculated IT diagram for boron steel using equation (Eq. 2) for each product structure and the data points indicate the determined experimental values for the starting and final transformations during isothermal heat treatments.

The actual temperature variation is continuous cooling rather than isothermal variation. But austenite transformation under $M_s$ temperature can develop a partial

transformation of bainite. By applying Scheil superposition principle (Scheil, 1935), the actual continuous cooling transformation can be calculated by isothermal transformation model. Here the time period was discretized based on the assumption that within each time step is $\Delta t$ at constant temperature involving isothermal transformation. For the corresponding constant $T_i$, were parameters $b_i$, $n_i$ and $\tau_i$ (transformation starting time, i.e. incubation period). By dividing the time step $\Delta t$ by incubation period $\tau_i$, increment of inoculation rate $\Delta E_i$ was the volume transformation during the former time step $V_i$. By substituting it into equation (Eq. 4) then the time period was obtained for the volume transformation reaching $V_i$ under $T_{i+1}$ isothermal transformation condition that is virtual time $t_{i+1}$ as described below.

$$t_{i+1} = \left[\frac{-ln(1-V_i)}{k_{i+1}}\right]^{\frac{1}{n_{i+1}}} \tag{4}$$

The microstructures were calculated from arrays {T (t)} and {V (t)} during the simulation period. Equations (Eq. 5 to Eq. 9) described below were included in the computer algorithm.

$$Vf_{max} = \left(\frac{0.8-C}{0.8}\right)^{-1} + \left(\frac{0.8-C}{0.8}\right)^{-1} \tag{5}$$

$$Vf = \sum_{i=1}^{n} -Kf \times Nf \times t^{Nf-1} \times e^{-Kf \times t^{Nf}} \times (1 - Vf_{max}) \tag{6}$$

$$Vp = \sum_{i=1}^{n} -Kp \times Np \times t^{Np-1} \times e^{-Kp \times t^{Np}} \times (1 - Vf) \tag{7}$$

$$Vb = \sum_{i=1}^{n} -Kb \times Nb \times t^{Nb-1} \times e^{-Kb \times t^{Nb}} \times (1 - Vf - Vp) \tag{8}$$

$$Vm = 1 - e^{-\beta \times (Tm_{start} - T)} \times (1 - Vf - Vp - Vb) \tag{9}$$

where: $Vf$ is the volume of ferite phase, $Vp$ is the volume of pearlite phase, $Vb$ is the volume of bainite phase, $Vm$ is the volume of martensite phase, $Kf$ ($Kp$ and $Kb$) are the overall rate constant of feritic, pearlitic and bainitic transformation that generally depends on temperature, $Nf$ ($Np$ and $Nb$) are the Avrami's exponent for feritic, pearlitic and bainitic transformation that depends on temperature, $t$ is the time, $T$ is the temperature, $T_{mstart}$ is the temperature martensite start transformation and $\beta$ is the coefficient of martensite transformation volume that depends on temperature.

The structure composition of steel cooling depends on the actual hardness defined as:

$$HV = V_P \times HV_P + V_B \times HV_B + V_M \times HV_M \quad (10)$$

Amount of phases proportion is an equal unity defined by (Li et al., 2001; Liu et al., 2003; Pietrzyk & Kuziak, 2011; Xie et al., 2013) as:

$$HV_M = 127 + 949 \times C + 27 \times Si + 8 \times Ni + 16 \times Cr + 21 \times lnV_r \quad (11)$$

$$\begin{aligned} HV_B = -323 &+ 185 \times C + 330 \times Si + 153 \times Mn + 65 \times Ni + 144 \\ &\times Cr + 191 \times Mo \\ &+ (89 + 53 \times C - 55 \times Si - 22 \times Mn - 10 \times Ni - 20 \\ &\times Cr - 33 \times Mo) \times lnV_r \end{aligned} \quad (12)$$

$$\begin{aligned} HV_{F,P} = 42 &+ 233 \times C + 53 \times Si + 30 \times Mn + 12.6 \times Ni + 7 \times Cr \\ &+ 19 \times Mo \\ &+ (10 - 19 \times Si + 4 \times Ni + 8 \times Cr + 130 \times V) \times lnV_r \end{aligned} \quad (13)$$

where: *C*, *Si*, *Mn* and others represent different kinds of chemical elements respectively (wt.%); $V_r$ represents cooling speed at 700 °C (°C $h^{-1}$).

From Eq. 10, it is not difficult to predict fraction of phases if the hardness of cooling microstructure and the hardness of microstructure constituents' are separately known (Eq. 11 to 13). Results of austenite decomposition depend on the chemical composition and steel history. The characteristic cooling time relevant for structure transformation for most steel is the time $t_{8\text{-}5}$. The characteristic cooling time was determined through series of algorithm where an average value of heat gradient between500 °C and 800 °C was found as illustrated in (Fig. 2).

The calculation of hardness was done by retrieving the temperature of nodes file. The analysis was performed for N nodes corresponding to the mesh of model. The temperature parameters of the nodes of the model were introduced (inlet) into the calculation of the volumetric representation of ferrite, pearlite, bainite and martensite.

In each step the temperature difference between the node in time was compared with the possible formation (or can be written as nuclei) parameters relevant phase (temperature and time dependence of TT diagram, for the structure formation) Fig. 2. The volume phase of the lower temperature node of ferrite formation (Ac3) was described by Eq. 6 whiles if that of pearlite formation (Ac1) with higher temperature node but higher than bainite formation was given by Eq. 7. On the other hand, the volume phase of bainite formation with temperature node higher than martensite was defined by Eq. 8 and that of volume phase of martensite formation with lower temperature node was given by Eq. 9. Equation (Eq. 10) was used to calculate the total hardness of individual phases. Data were saved to a new file that has the same format as the source file which can be opened in the program Paraview. This cycle was repeated for each temperature nodes file to the last file with nodes.

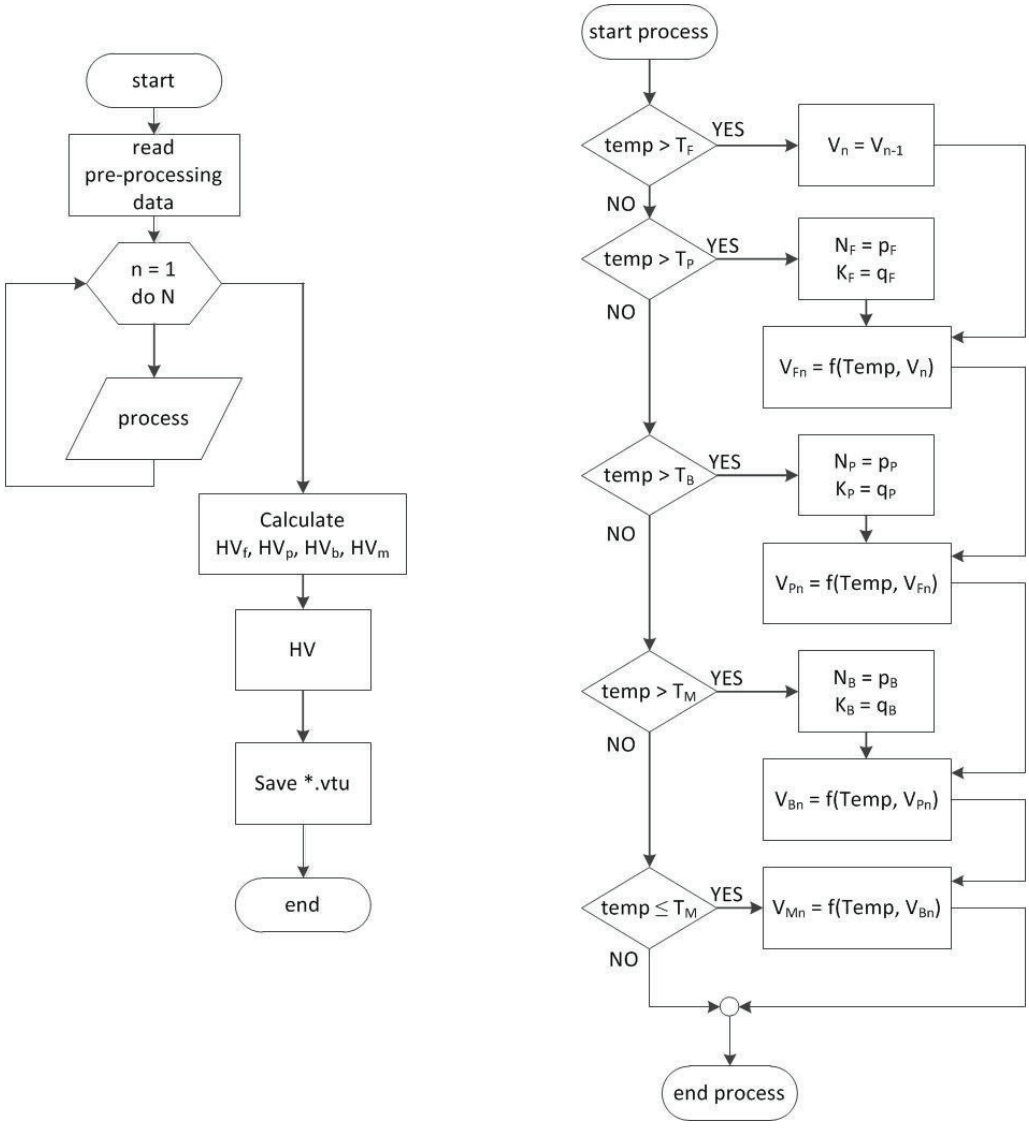


**Figure 2.** Schematic of computer algorithm.

## RESULTS AND DISCUSSION

A mathematical model for the prediction of temperature of nonstationary heat transfer in relation to time of a quenched steel chisel was used. The initial properties of the steel and the boundary conditions were used in the model to verify the results using ElmerFem software. The temperature distribution and curves are illustrated in Figs 3 and 4 respectively.

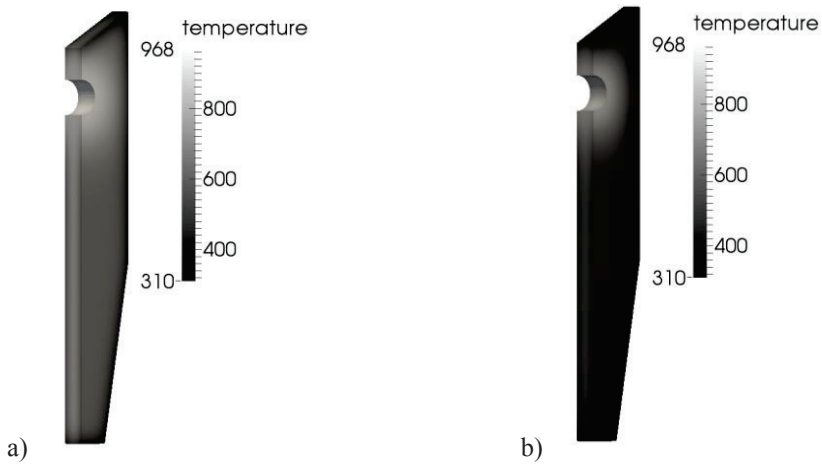


**Figure 3.** Temperature distribution of a quenched chisel at 5 (a) and 15 (b) sec cooling in water.

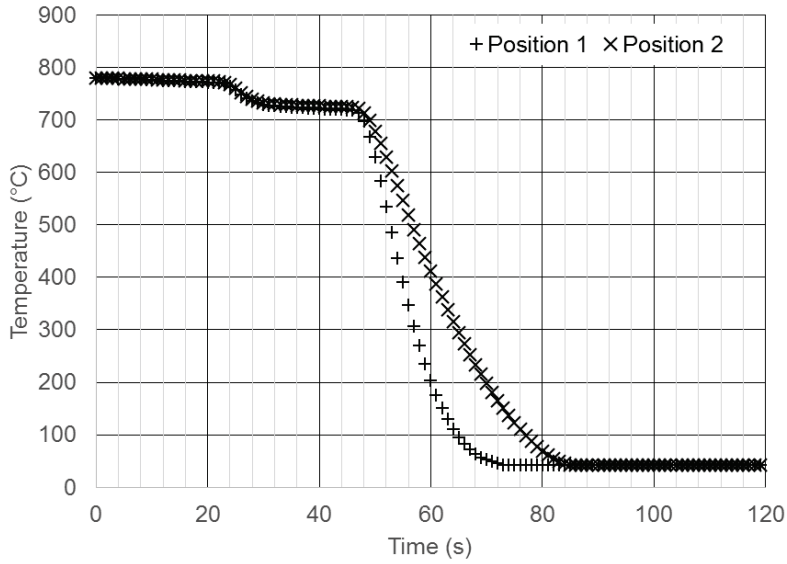


**Figure 4.** Cooling curve of modeled chisel in two positions (near to hole – position 1 and far from hole – position 2).

Distribution of microstructure fields of the quenched chisel is presented in Fig. 5 whiles the hardness fields of the quenched chisel is shown in Fig. 6. The results showed a good distribution of softer microstructure around a hole in chisel, where their sharp notches were often placed by cracked initiation (Liu et al., 2003; Liu et al., 2004; Guo et al., 2009; Chen et al., 2012). The problem with low fracture toughness of the martensite structure was solved using lower heat flux around hole as well as technological solution using ceramics holders in hole and around hole.

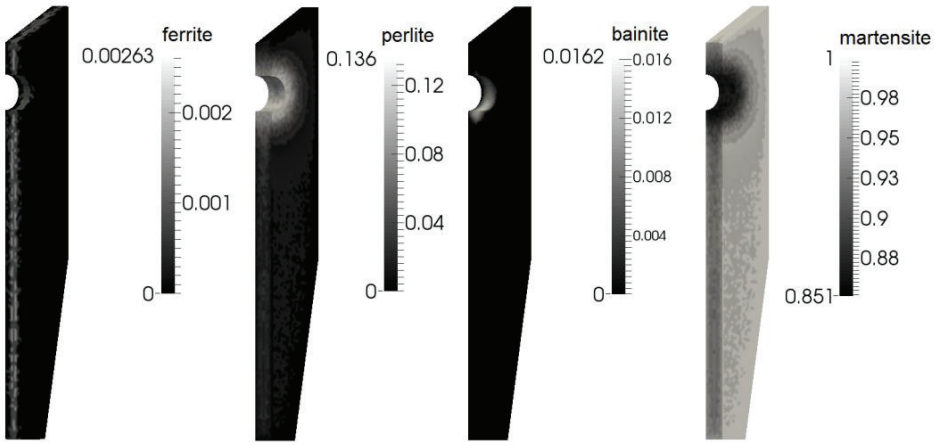


**Figure 5.** Distribution of microstructure fields of the quenched chisel – high boron steel B1.

Using models of steel B2 and Boron 27 produced two microstructure mixtures namely martensitic and ferritic. These mixtures are non homogenous because ferrite is usually acicular on the boundary of austenite (Liu et al., 2004). They are also more brittle than other mixtures of microstructure in the steel and they have a high degree of damage of the intercrytalline fracture (Jam et al., 2014). Therefore the martensitic structure get better wear resistant properties than softer microstructures (Chotěborský, 2013; Chotěborský & Hrabě, 2013). Samples of chisel were not analyzed on microstructure. In this article are discussed only circle sample (3 pieces of each steel) tested steels after heat treatment cycle of similar properties like modeled microstructure.

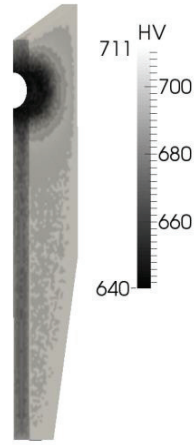


**Figure 6.** Hardness field of high boron steel B1 after quenching in water.

But microstructure volume of tested steel was different after heat treatment in comparison with modeled samples. Errors were observed from the modeling of the specific heat coefficient, heat flux, computed transformation diagrams. Equations (Eqs 10 to 13) increased the difference between modeling and experimental results. Also real chemical composition, grain size, number of crystal lattice and thermal history directly influenced the results of experimental steel as well as the difference between modeling and experimental results. These analyses showed errors around 15% volume of microstructure phases similar to published results (Liu et al., 2003; Huiping et al., 2007; Lee et al., 2010; Lee et al., 2013).

## CONCLUSIONS

A simply method for axisymmetric modeling of heat FEM in agriculture tools is possible.

JMAK equation can be used for prediction of microstructure.

A relatively good relationship between modeled and measured microstructures was observed compared to modeled and measured volume of microstructural phases.

Experimental and modeled results showed errors around 15% of predicted hardness. Hardness is one of the interested mechanical properties but the presented errors were very high. These models setup can be useful for different technological procedures with heat cycle during processing and for prediction of microstructure.

## REFERENCES


Archambault, P. & Azim, A. 1995. Inverse resolution of the heat-transfer equation: application to steel and aluminum alloy quenching. *Journal of Materials Engineering and Performance* **4**(6), 730–736.

Avrami, M. 1939a. J. Chem. Phys. 7 (pp. 1103–1109).

Avrami, M. 1939b. Kinetics of phase change. I: General theory. *The Journal of Chemical Physics*, *7*(12), 1103–1112.

Avrami, M. 1940a. J. Chem. Phys. 8 (pp. 212–224).

Avrami, M. 1940b. Kinetics of phase change. II Transformation-time relations for random distribution of nuclei. *The Journal of Chemical Physics*, *8*(2), 212–224.

Buczek, A. & Telejko, T. 2013. Investigation of heat transfer coefficient during quenching in various cooling agents. *International Journal of Heat and Fluid Flow* **44**, 358–364.

Carlone, P., Palazzo, G.S. & Pasquino, R. 2010. Finite element analysis of the steel quenching process: Temperature field and solid–solid phase change. *Computers & Mathematics with Applications* **59**(1), 585–594.

Çetinel, H., Toparlı, M. & Özsoyeller, L. 2000. A finite element based prediction of the microstructural evolution of steels subjected to the Tempcore process. *Mechanics of Materials* **32**(6), 339–347.

CSC - IT Center for Science (CSC). (2013). Elmer finite element software. Retrieved from http://www.csc.fi/english/pages/elmer

Fall, A., Regnier, M.C., Manga, P.-S., Ramassamy, C., Tonnon, E., Romberger, C. & Xiao Yuefa, J. 2011. Tools for continuous improvement of the plate quenching process. *Revue de Métallurgie* **108**(5), 313–321.

Ferguson, B.L., Li, Z. & Freborg, A.M. 2005. Modeling heat treatment of steel parts. *Computational Materials Science* **34**(3), 274–281.

Guo, Z., Saunders, N., Miodownik, P. & Schille, J.P. 2009. Modelling phase transformations and material properties critical to the prediction of distortion during the heat treatment of steels. *International Journal of Microstructure and Materials Properties* **4**(2), 187.

Hasan, H.S., Peet, M.J., Jalil, J.M. & Bhadeshia, H.K.D.H. 2010. Heat transfer coefficients during quenching of steels. *Heat and Mass Transfer* **47**(3), 315–321.

Huiping, L., Guoqun, Z., Shanting, N. & Chuanzhen, H. 2007. FEM simulation of quenching process and experimental verification of simulation results. *Materials Science and Engineering: A*, **452-453**, 705–714.

Chen, J., Mo, W., Wang, P. & Lu, S. 2012. Effects of tempering temperature on the impact toughness of steel 42CrMo. *Jinshu Xuebao/Acta Metallurgica Sinica* **48**(10), 1186–1193.

Chotěborský, R. 2013. Effect of heat treatment on the microstructure, hardness and abrasive wear resistance of high chromium hardfacing. *Research in Agricultural Engineering* **59**(1), 23–28.

Chotěborský, R. & Hrabě, P. 2013. Effect of destabilization treatment on microstructure, hardness and abrasive wear of high chromium hardfacing. *Research in Agricultural Engineering* **59**(4), 128–135.

Jam, J.E., Abolghasemzadeh, M., Salavati, H. & Alizadeh, Y. 2014. The Effect of Notch Tip Position on the Charpy Impact Energy for Bainitic and Martensitic Functionally Graded Steels. *Strength of Materials* **46**(5), 700–716.

Johnson, A.W. & Mehl, E.R. (1939). Trans. AIME 135 (pp. 416–458).

Kirkaldy, J.S. 2007. Flux-independent theory of nonlinear diffusion for Vegard's law solutions. *Materials Science and Engineering: A*, **444**(1-2), 104–111.

Kolmorgorov, A.N. 1937. Izv. Akad. Nauk. SSSR. Ser. Matem (pp. 355–359).

Lee, S.-J., Matlock, D.K. & Van Tyne, C.J. 2013. Comparison of two finite element simulation codes used to model the carburizing of steel. *Computational Materials Science* **68**, 47–54.

Lee, S.-J., Pavlina, E.J. & Van Tyne, C.J. 2010. Kinetics modeling of austenite decomposition for an end-quenched 1045 steel. *Materials Science and Engineering: A*, **527**(13–14),

Li, X., Miodownik, A.P. & Saunders, N. 2001. Simultaneous calculation of mechanical properties and phase equilibria. *Journal of Phase Equilibria* **22**(3), 247–253.

Liu, C.C., Xu, X.J. & Liu, Z. 2003. A FEM modeling of quenching and tempering and its application in industrial engineering. *Finite Elements in Analysis and Design* **39**(11), 1053–1070.

Liu, D., Xu, H., Yang, K., Bai, B. & Fang, H. 2004. Effect of bainite/martensite mixed microstructure on the strength and toughness of low carbon alloy steels. *Jinshu Xuebao/Acta Metallurgica Sinica* **40**(8), 882–886.

Malinowski, Z., Telejko, T. & Hadała, B. 2012. Influence of Heat Transfer Boundary Conditions on the Temperature Field of the Continuous Casting Ingot. *Archives of Metallurgy and Materials* **57**(1).

Marder, A.R. & Goldstein, J. 1984. Phase Transformations in Ferrous Alloys: Proceedings of an International Conference, 411.

Pietrzyk, M. & Kuziak, R. 2011. Computer aided interpretation of results of the Jominy test. *Archives of Civil and Mechanical Engineering* **11**(3), 707–722.

Scheil, E. 1935. Archiv f. Eisenhűttenw. 8, pp. 565–567.

Sinha, V.K., Prasad, R.S., Mandal, A. & Maity, J. 2007. A Mathematical Model to Predict Microstructure of Heat-Treated Steel. *Journal of Materials Engineering and Performance* **16**(4), 461–469.

Smoljan, B. 2006. Prediction of mechanical properties and microstructure distribution of quenched and tempered steel shaft. *Journal of Materials Processing Technology* **175**(1–3), 393–397.

Telejko, T. 2004. Analysis of an inverse method of simultaneous determination of thermal conductivity and heat of phase transformation in steels. *Journal of Materials Processing Technology* **155–56**, 1317–1323.

Xie, J. Bin, Wu, C.C., Fan, J., Fu, M. & Hu, D.F. 2013. Numerical Simulation on the Temperature Field of Steel 1045 Quenched by Different Hardening Media. *Applied Mechanics and Materials* **444–445**, 1222–1228.